ELECTRONIC SUPPLEMENTARY INFORMATION

High-performance Na ion cathodes based on ubiquitous and reversible O redox reaction

M. Hussein N. Assadi,[a,b,*] Marco Fronzi,[c,d] Mike Ford[c] and Yasuteru Shigeta[a]

[a]Center for Computational Sciences, University of Tsukuba, Tennodai 1-1-1, Tsukuba, Ibaraki 305-8577, Japan.

[b]Center for Green Research on Energy and Environmental Materials (GREEN), National Institute for Materials Science (NIMS), 1-1 Namiki, Tsukuba, Ibaraki 305-0044, Japan.

[c]International Research Centre for Renewable Energy, State Key Laboratory of Multi- phase Flow in Power Engineering, Xi'an Jiaotong University, Xi'an 710049, Shaanxi, China.

[d]School of Mathematical and Physical Science, University of Technology Sydney, Ultimo 2007, New South Wales 2007, Australia.

[*]Email: h.assadi.2008@ieee.org

1. Additional Computational Settings

The pseudopotentials used in calculations contained the following electrons: $2s^2 2p^4$ for O; $2p^6 3s^1$ for Na, $4p^6 4d^4 5s^1$ for Nb, $4p^6 4d^5 5s^1$ for Mo; $4p^6 4d^{10}$ for Pd; and $4d^{10} 5s^1$ for Ag. The specific capacity ($Q_{Theoretical}$) in mAh/g was calculated according to the following formula:

$$Q_{Theoretical} = \frac{nF}{3600 M_{Molecular}} \qquad \text{Equation S1.}$$

Here, n is the extracted charge, $\mathcal{F}$ is the Faraday constant (96485.3329 sA/mol), and $M_{Molecular}$ is the molecular weight in g/mole. The energy density was calculated by multiplying the specific capacity in the cell voltage.

2. Structural Details

The Na_1NbO_2 and Na_3AgO_2 compounds have been previously synthesised and characterised [1,2]. Tables S1 and S2 present the calculated and experimental lattice parameters for these two compounds. The calculated and measured lattice parameters differ only by ~1% indicating excellent convergence of the DFT calculation within the GGA+U framework.

Table S1. The calculated and experimental lattice parameters of Na_1NbO_2.

Na_1NbO_2	Calculated	Experimental
Lattice Group	194 ($P6_3/mmc$)	194 ($P6_3/mmc$)
a (Å)	3.013	2.955
b (Å)	3.013	2.955
c (Å)	11.708	11.647
α (°)	90.000	90
β (°)	90.000	90
γ (°)	120.000	120

Table S2. The calculated and experimental lattice parameters of Na_3AgO_2.

Na_3AgO_2	Calculated	Experimental
Lattice Group	72 ($Ibam$)	72 ($Ibam$)
a (Å)	5.525	5.463
b (Å)	11.031	10.926
c (Å)	6.002	5.926
α (°)	90.000	90
β (°)	90.000	90
γ (°)	90.000	90

Monoclinic Na_2MoO_4 has been synthesised [3]. Its structure, however, has not been fully characterised yet. We, nonetheless, present a comparison between the calculated Na_2MoO_4 lattice parameters and the lattice parameter of the isostructural monoclinic K_2MoO_4 [4] in Table S3. The lattice constants of Na_2MoO_4 are ~5% smaller than those of K_2MoO_4. This shrinkage can be attributed to the smaller ionic radius of Na^+ compared to that of K^+.

Table S3. Comparison between the calculated lattice parameters of Na_2MoO_4 with the experimental lattice parameters of K_2MoO_4.

Na_2MoO_4	Calculated Na_2MoO_4	Experimental K_2MoO_4
Lattice Group	12 ($C2/m$)	12 ($C2/m$)
a (Å)	11.692	12.348
b (Å)	5.945	6.081
c (Å)	6.942	7.538
α (°)	90.000	90
β (°)	117.647	115.74
γ (°)	90.000	90

$Na_4Zr_5O_{12}$ and $Na_1Pd_2O_3$ have not yet been synthesis. We modelled these compounds after the synthesised and well-characterised $K_4Zr_5O_{12}$ and KPd_2O_3 [5-7]. Tables S4 and S5 present a comparison between the Na based and K based compounds. The c value is 2.01% shorter in $Na_4Zr_5O_{12}$ than in $K_4Zr_5O_{12}$. The difference is more profound in the palladate compounds as the *c* is 11.12% smaller in sodium palladate than in potassium palladate.

Table S4. Comparison between the calculated lattice parameters of $Na_4Zr_5O_{12}$ with the experimental lattice parameters of $K_4Zr_5O_{12}$.

	$Na_4Zr_5O_{12}$ (Calculated)	$K_4Zr_5O_{12}$ Experimental
Lattice Group	164 ($P\bar{3}m1$)	164 ($P\bar{3}m1$)
a (Å)	5.855	5.821
b (Å)	5.855	5.821
c (Å)	10.652	10.437
α (°)	90.000	90
β (°)	90.000	90
γ (°)	120.000	120

Table S5. Comparison between the calculated lattice parameters of $Na_1Pd_2O_3$ with the experimental lattice parameters of $K_1Pd_2O_3$.

	$Na_1Pd_2O_3$ (Calculated)	$K_1Pd_2O_3$ (Experimental)
Lattice Group	160 ($R3mR3m$)	160 ($R3m$)
a (Å)	6.130	6.073
b (Å)	6.130	6.073
c (Å)	16.897	18.777
α (°)	90.000	90
β (°)	90.000	90
γ (°)	120.000	120

Since $Na_4Zr_5O_{12}$ and $Na_1Pd_2O_3$ have not been synthesised yet, we examined their stability against the binary oxides they may decompose to. The results are presented in Table S6. Negative formation enthalpy (ΔH) indicates the stability of the ternary compounds. According to Table S6, both $Na_4Zr_5O_{12}$ and $Na_1Pd_2O_3$ were found energetically stable against decomposing into the competing binary oxides.

Table S6. The formation enthalpy (ΔH) of the ternary oxides with respect to the binary oxides.

compound	ΔH(eV/u.f.)	Competing oxide phases
$Na_4Zr_5O_{12}$	−8.241	$5ZrO_2+2Na_2O$
$Na_1Pd_2O_3$	−4.177	$2PdO+½Na_2O+¼O_2$

3. Choice of Functional

The conventional and popular general gradient approximation (GGA) is known to delocalise overly the *d* states and underestimate bang gaps of the transition metal (TM) oxides [8]. Since the localisation effects are stronger for 3d electrons, these problems manifest most adversely in 3d TM oxides. However, in the 4d TM oxides we studied here, localisation effects are rather smaller, and the shortcoming of the GGA method can be mitigated by introducing a modest Hubbard term on the 4*d* electrons. In our work, we choose a U_{eff} value of 2 eV for all TM ions. The choice of a single value U_{eff} allowed us a straightforward comparison of the materials properties. This approach has been successfully applied to survey studies for Na_2TMO_3 [9], $NaTMO_2$ [10] and ZnO:TM [11] systems. In Figure S1, we present the DOS of the sodiated and desodiated compounds calculated under the GGA functional. For most of the compounds, the GGA DOS is approximately similar to the one calculated with GGA+U functional (Figure 3) indicating lack of strong localisation effects in the studied compounds. The only Noticeable difference occurs in $Na_{0.5}Pd_2O_3$ for which the position of the Fermi level is wrongly placed in the middle of the valence band in GGA calculations. Table S7, presents the half-cell voltages calculated with GGA functional and the GGA+U (U_{eff} = 2 eV). Evidently, GGA+U method introduces the necessary moderate correction with respect to the mere GGA method.

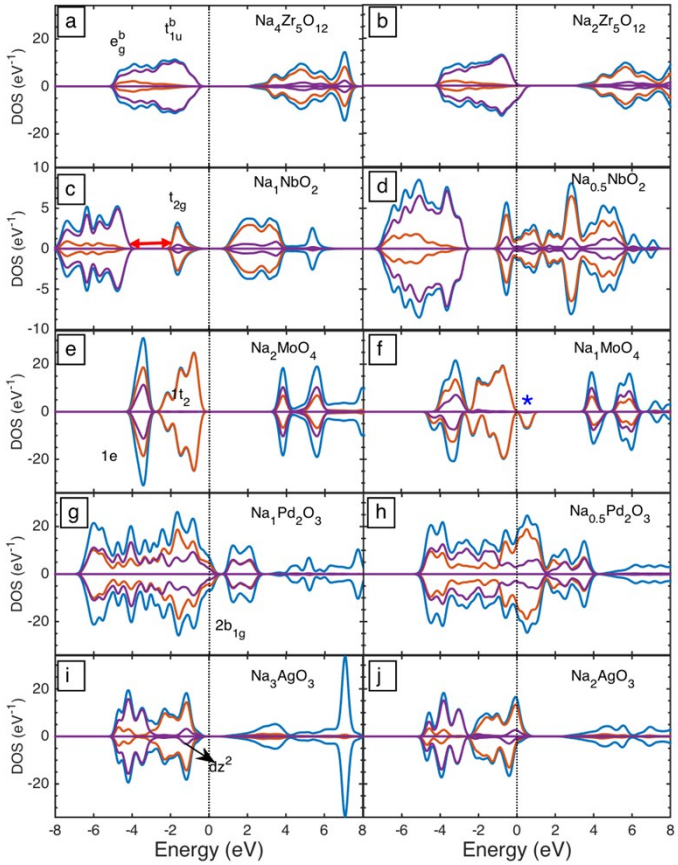

Figure S1. The total and partial density of states of the sodiated (left column) and desodiated compounds (right column) calculated with GGA method. Blue, purple and orange lines represent total, TM 4d and O 2p partial states respectively.

Table S7. Voltages calculated with GGA+U and GGA functionals.

	$Na_{4-x}Zr_5O_{12}$	$Na_{1-x}NbO_2$	$Na_{2-x}MoO_4$	$Na_{1-x}Pd_2O_3$	$Na_{3-x}AgO_2$.
Potential (V) GGA+U	3.583	2.476	4.743	2.630	2.398
Potential (V) GGA	3.790	2.247	4.369	2.666	2.314

To examine the how the DOS is influenced if we chose a higher U_{eff} value or higher level functional, we calculated the DOS of the Na_2MoO_4 compound with U_{eff} = 3.7 eV and the hybrid HSE06 functional [12,13] with a mixing parameter α = 0.2, presented in Figure S1(b) and (c) respectively. U_{eff} value of 3.7 eV was used for Na_2MoO_4 in Materials Project (materialsproject.org). Furthermore, Mo oxides are known to exhibit particularly strong localisation effect [14]. As we can see in Figure 2S, the dominance of O 2p states near the valence band maximum is a preserved feature for all functional used. Furthermore, the calculated bandgap (E_g) does not strongly depend on the functional chosen indicating that U_{eff} value we used in the calculation was adequate for these 4d TM oxides. Consequently, U_{eff}= 2 eV for calculating the voltages is adequately robust and efficient.

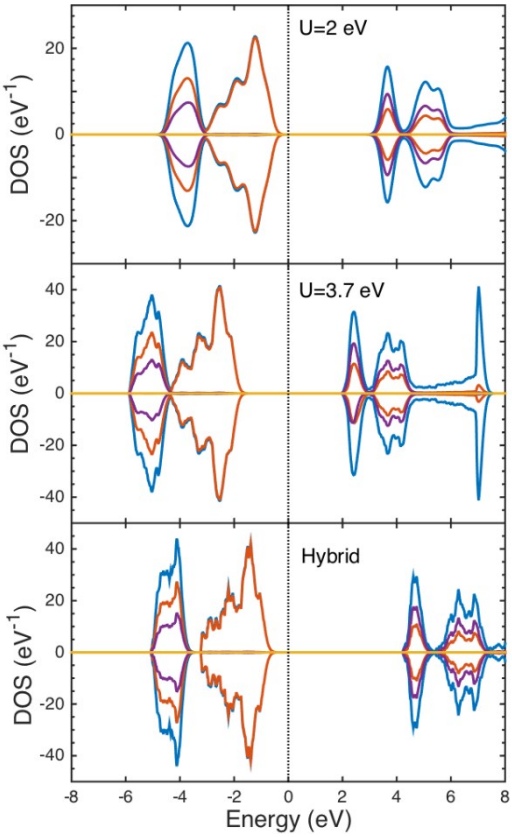

Figure S2. The total and partial density of states of the Na_2MoO_4 compound calculated with various functionals. Blue, purple and orange lines represent total, O 2p and TM 4d partial states respectively.

4. Desodiation Process in $Na_{4-x}Zr_5O_{12}$ and $Na_{3-x}AgO_2$

Calculating the equilibrium voltage using Equation 1 requires the free energy of the thermodynamically stable structures of the sodiated and desodiated compounds. Since the entropic contribution is small and hence neglected in our calculations, we used the total DFT energy in place of the free energy. When there are different possibilities for Na vacancy formation or their arrangements, care should be taken to ensure that the most stable configuration is considered for calculating the voltage. Accordingly, we calculated the voltages based on the most stable V_{Na} configuration in $Na_{4-x}Zr_5O_{12}$ and $Na_{3-x}AgO_2$ compounds in which there are two distinct V_{Na}s. Comparing the formation energy of V_{Na}s, however, identifies the most stable configuration at the early stages of the desodiation. To confirm that sodium vacancies from 2d Wyckoff site in $Na_{4-x}Zr_5O_{12}$ and 4b Wyckoff in $Na_{3-x}AgO_2$ are still the most stable in fully desodiated compounds, we calculated the total energy of hypothetical fully desodiated $Na_2Zr_5O_{12}$ and Na_2AgO_2 compounds in which Na ions from alternative 2c and 8g sites were extracted respectively. We found that the total energy of $Na_2Zr_5O_{12}$ rose by 0.40 eV per unit formula and the total energy of Na_2AgO_2 rose by 1.44 eV per unit formula when alternative Na sites were completely vacated instead of those forming most stable vacancies.

References

1 Hans-Friedrich, R., Gerd, M., Zhiwei, H. & Günter, K. Synthesis, structure, and X-ray absorption spectra of Li_xNbO_2 and Na_xNbO_2 ($x \leq 1$). *Z. Anorg. Allg. Chem.* **619**, 1369–1373, doi:doi:10.1002/zaac.19936190808 (1993).

2 Klassen, H. & Hoppe, R. Alkalioxoargentate(I). Über Na_3AgO_2. *Z. Anorg. Allg. Chem.* **485**, 92–100, doi:doi:10.1002/zaac.19824850109 (1982).

3 Busey, R. H. & Keller, O. L. Structure of the Aqueous Pertechnetate Ion by Raman and Infrared Spectroscopy. Raman and Infrared Spectra of Crystalline $KTcO_4$, $KReO_4$, Na_2MoO_4, Na_2WO_4, $Na_2MoO_4 \cdot 2H_2O$, and $Na_2WO_4 \cdot 2H_2O$. *J. Chem. Phys.* **41**, 215–225, doi:10.1063/1.1725625 (1964).

4 Gatehouse, B. M. & Leverett, P. Crystal structure of potassium molybdate, K_2MoO_4. *J. Chem. Soc. A*, 849–854, doi:10.1039/J19690000849 (1969).

5 Gatehouse, B. M. & Nesbit, M. C. The crystal structure of the 2:5 phase in the K_2O-ZrO_2 system: $K_4Zr_5O_{12}$, a compound with octahedral and trigonal prismatic zirconium(IV) coordination. *J. Solid State Chem.* **31**, 53–58, doi:https://doi.org/10.1016/0022-4596(80)90007-9 (1980).

6 Wang, Q. *et al.* Preparation and catalytic activity of $K_4Zr_5O_{12}$ for the oxidation of soot from vehicle engine emissions. *J. Ind. Eng. Chem.* **16**, 68–73, doi:10.1016/j.jiec.2010.01.019 (2010).

7 Panin, R. V. *et al.* Ordering of Pd^{2+} and Pd^{4+} in the mixed-valent palladate KPd_2O_3. *Inorg. Chem.* **49**, 1295–1297, doi:10.1021/ic902187a (2010).

8 Pribram-Jones, A., Gross, D. A. & Burke, K. DFT: A Theory Full of Holes? *Annu. Rev. Phys. Chem.* **66**, 283–304, doi:10.1146/annurev-physchem-040214-121420 (2015).

9 Assadi, M. H. N., Okubo, M., Yamada, A. & Tateyama, Y. Oxygen redox in hexagonal layered Na_xTMO_3 (TM = 4d elements) for high capacity Na ion batteries. *J. Mater. Chem. A* **6**, 3747–3753, doi:10.1039/C7TA10826E (2018).

10 Assadi, M. H. N. & Shigeta, Y. Dominant role of orbital splitting in determining cathode potential in O3 $NaTMO_2$ compounds. *J. Power Sources* **388**, 1–4, doi:https://doi.org/10.1016/j.jpowsour.2018.03.056 (2018).

11 Gopal, P. & Spaldin, N. A. Magnetic interactions in transition-metal-doped ZnO: An ab initio study. *Phys. Rev. B* **74**, 094418, doi:10.1103/PhysRevB.74.094418 (2006).

12 Heyd, J., Scuseria, G. E. & Ernzerhof, M. Hybrid functionals based on a screened Coulomb potential. *J. Chem. Phys.* **118**, 8207–8215, doi:10.1063/1.1564060 (2003).

13 Heyd, J., Scuseria, G. E. & Ernzerhof, M. Erratum: “Hybrid functionals based on a screened Coulomb potential” [J. Chem. Phys. 118, 8207 (2003)]. *J. Chem. Phys.* **124**, 219906, doi:10.1063/1.2204597 (2006).

14 Lutfalla, S., Shapovalov, V. & Bell, A. T. Calibration of the DFT/GGA+U Method for Determination of Reduction Energies for Transition and Rare Earth Metal Oxides of Ti, V, Mo, and Ce. *J. Chem. Theory Comput.* **7**, 2218-2223, doi:10.1021/ct200202g (2011).